COMSOL CONFERENCE 2023 MUNICH

Numerical Optimization of Electroactive Actuator Position for Optical Mirror Applications

K. THETPRAPHI[1,3], V. BRUYERE[2], D. AUDIGIER[1], J.F. CAPSAL[1], P. NAMY[2], G. MORETTO[3]
1. Univ Lyon, INSA-Lyon, LGEF, EA682, F-69621, Villeurbanne, France
2. SIMTEC, 5 rue Felix Poulat, Grenoble, France
3. Centre de Recherche Astrophysique de Lyon (CRAL), 9 avenue Charles André, 69230 Saint-Genis-Laval, France

Abstract
Electroactive actuators are widely used in precision optical systems to control the position and shape of optical elements, such as telescope mirrors. However, the optimal position of the electroactive actuator for a given optical mirror design is not obvious, and numerical optimization techniques can be employed to find the optimal solution. To control the local curvature of the mirror and to define the objective to minimize in the optimization procedure, a first distributed ODE is implemented. In a second step, a mechanical model is developed to compute the mirror displacement as a function of the force applied by the piezoelectric actuators. Finally, an optimization procedure is used to minimize the local curvature by controlling the intensity and distribution of the electromechanical force. The optimized results show a strong interest in the use of this technology to minimize the initial defects related to the manufacturing of the mirror or the defects during use related to the gravity creep.

Keywords: Optimization, Curvature Computation, Electroactive actuators, Active Optics

Introduction

Exolife-Finder (ELF), which is slated to be the largest telescope ever built, was unveiled by Live-Mirror consortium as part of an interdisciplinary research project. This telescope's innovative concept relies on utilizing the power of advanced Electroactive Polymer (EAP) actuators. These actuators will serve as an electromechanical spring integrated onto the mirror's rear surface, avoiding any contact with the optical surface itself. This innovative approach transforms the EAP actuator into a superior optical shape correction system, surpassing the capabilities of conventional actuators.

Recently, we investigate the optical surface using Fizeau-type laser interferometer (ZYGO Verifire™). The sample's surface profile can be acquired through static fringe interpretation analysis, achieved by employing a Fourier transform on the intensity distribution. This transformation is followed by a transition to the spatial frequency domain facilitated by the software interface. Utilizing the phase calculation-driven fringe projection technique, we can then generate a three-dimensional surface plot of the actual mirror. Determining the optimal actuator distribution in response to actual mirror surface roughness may not be straightforward. Numerical optimization methods can be used in conjunction with input from the actual mirror's surface to get the optimal solution.

Modeling and Governing Equations

Each “physics” used in COMSOL Multiphysics® is detailed with the different assumptions used in this work. Three major aspects are detailed in this paper: the calculation of the local curvature, the description of the mechanical problem and the optimization methods.

Local Curvature Computation

As detailed above, the experimental measurement gives the height of the glass disc (with normal vector $\boldsymbol{y}$) as a function of space. This is imported into COMSOL Multiphysics® from a .txt file using an interpolation function $h(x,z)$. A representation of a test measurement is shown in Figure 1.

In order to master the optical aspects of the mirror, control of the local curvature is essential. The first objective is therefore to calculate this local surface curvature accurately. It can be done in COMSOL Multiphysics® through several approaches.

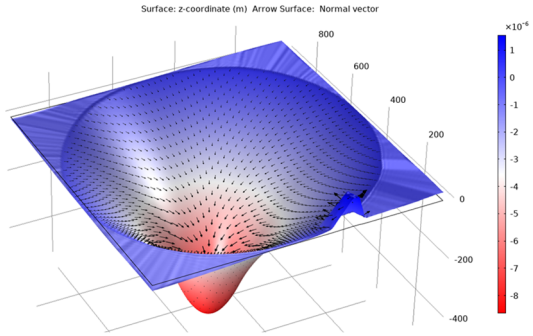

Figure 1. Imported Height

One of the methods tested in this work is the use of the “Parametric Surface” tool in the geometry kernel. It consists of a geometric description of the surface based on the imported height. A Coefficient Form

Boundary PDE is added to define the variable of interest w:

$$w = h(x,z) \qquad \textit{Eq. 1}$$

The local curvature can then be computed using the tangential expression of the second derivatives:

$$\rho_{geom} = (I - \boldsymbol{n}\boldsymbol{n}^T)\left(\frac{\partial^2 w}{\partial x^2} + \frac{\partial^2 w}{\partial z^2}\right) \qquad \textit{Eq. 2}$$

with I the identity tensor and $\boldsymbol{n}$ the normal vector.

This approach provides good accuracy with a fine mesh but is difficult to couple with the following mechanical problem. Another approach has also been used to estimate the local curvature. The geometry is only a flat surface here, and a Coefficient Form PDE is defined. The following equation is then solved:

$$\lambda \Delta w_2 + w_2 = h(x,z) \qquad \textit{Eq. 3}$$

with λ a tunning parameter, w_2 the resulting height and $h(x,z)$ the imported interpolated height.

The local curvature can then be defined with "classical" second derivatives by:

$$\rho = \frac{\partial^2 w_2}{\partial x^2} + \frac{\partial^2 w_2}{\partial z^2} \qquad \textit{Eq. 4}$$

The influence of the tuning parameter will be studied in the numerical section of this paper to validate the approach. Both approaches will also be compared.

Mechanical Problem

The aim of the work is to determine the position of the actuators enabling precise control of the curvature of the mirror. In a previous work [1], relationships between the electrical potential, the thickness of the actuators, their electrical properties and the resulting stress were obtained. The model developed here does not consider the electro-mechanical coupling and aims to describe a simplified mechanical problem for which a force (of an order of magnitude comparable to that generated by the actuators) is applied to each actuator.

The 3D geometry of the glass and flange is imported and shown in Figure 2. The ZYGO measures the height of the surface from the top, and the actuators are positioned on the underside (bottom, Figure 2). The position and the number of actuators are parametrized to treat different study cases from no actuator for the topology optimization to more than 50 for parametric optimization.

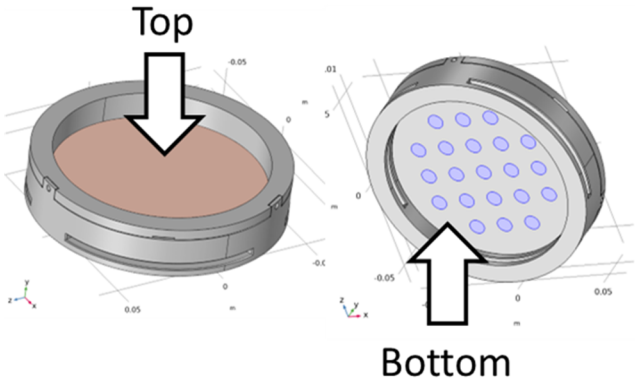

Figure 2. Geometry of the glass and flange (left) and Actuators locations (right)

The mechanical problem consists in solving the divergence of the stress tensor to obtain the resulting displacement field, $\boldsymbol{u}$:

$$\nabla \cdot S = 0 \qquad \textit{Eq. 5}$$

where S is the stress tensor related to the elastic strain tensor, ε_{el}, by:

$$S = C : \varepsilon_{el} \qquad \textit{Eq. 6}$$

with $C = C(E,\nu)$ is the rigidity matrix with E the Young's modulus and ν the Poisson's ratio and

$$\varepsilon_{el} = \frac{1}{2}[(\nabla \boldsymbol{u})^T + \nabla \boldsymbol{u}] \qquad \textit{Eq. 7}$$

For each actuator, a boundary load is applied in the normal direction:

$$S \cdot \boldsymbol{n} = -p_i \boldsymbol{n} \qquad \textit{Eq. 8}$$

with p_i the pressure applied on the actuator i.

Optimization Procedure

Two different procedures have been developed in this work to study the feasibility and the relevance of each one. First of all, topologic optimization procedure is discussed. The aim is to determine the distribution of a load surface (representing a continuous actuator density) that minimizes the local curvature. This can be physically achieved by using actuators with complex shape, printed by additive manufacturing.

The applied pressure is defined on the bottom surface (see Figure 2) without any actuator. The load is function of an artificial material volume factor, θ, which acts as control variable in the optimization problem:

$$S \cdot \boldsymbol{n} = K_f * \theta(x,z)\boldsymbol{n} \qquad \textit{Eq. 9}$$

with K_f the order of magnitude of the pressure provided by one actuator.

The objective function is manually scaled and defined by the following integration on the top surface:

$$J = \iint \left(\rho_{init} - \rho(\theta)\right)^2 d\Gamma_{top} \qquad \textit{Eq. 10}$$

with ρ_{init} is the local curvature before applying the load (computed from equation 4), and $\rho(\theta)$ the current local curvature.
An MMA solver is used to solve the optimization problem. A filter type of Helmholtz is used with a hyperbolic tangent projection with a β projection slope [2].

In a second stage, the influence of a discrete distribution of actuators is studied. The objective is to obtain the best distribution of load on each actuator (geometrically defined), minimizing local curvature. Each actuator has then a parametrized constant load that should be a result of the optimization solver.
The following global objective is defined in the General Optimization procedure:

$$J = \iint \left(\rho_{init} - \rho(x,z)\right)^2 \qquad \textit{Eq. 11}$$

For each actuator i, a control variable is set to define a pressure p_i (see equation 8). Depending on the numbers of actuators, it can be very fastidious to do it manually. A Java algorithm has been developed to generalize it by using application builder.
Concerning the solver, the SNOPT method is used for this optimization procedure.

Numerical Validations

Mesh Convergence for Curvature Computations

As discussed above, different approaches have been evaluated to compute the local curvature. The influence of the mesh size has been studied for each of them and the results are shown here for the geometric approach.

A mapped mesh is used and the influence of the number of elements, $n_{element}$, on each edge of the square, is studied (Figure 3).

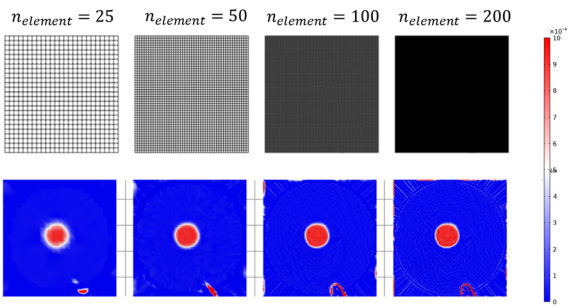

Figure 3. Meshes (top) and associated local curvature (bottom)

The computation of the curvature gives clearly more precise and sharper results with finer mesh. The required precision is reached for $n_{element} = 100$.

Concerning the second approach developed to compute the curvature, the influence of the λ parameter (tuning parameter) is studied to validate the accuracy of the method, with the same previous refined mesh. Summarized results are shown in Figure 4 through cut line as a function of x at $z = 0$ and with surfaces in Figure 5. The influence of the λ parameter is studied for different values in Figure 4. The geometric approach is defined as reference to compare the results.
The higher the λ parameter, the more important the Laplacian term (in equation 3), the smoother the results. For very low value of λ parameter ($\lambda < 1e-11$) the results are very noisy. With $\lambda = 1e-11$, results are in very good agreement with the geometrical approach (see Figure 4 and Figure 5). Results from another software (IDL code in Figure 5) have also been compared and a very good agreement is obtained with both approaches.

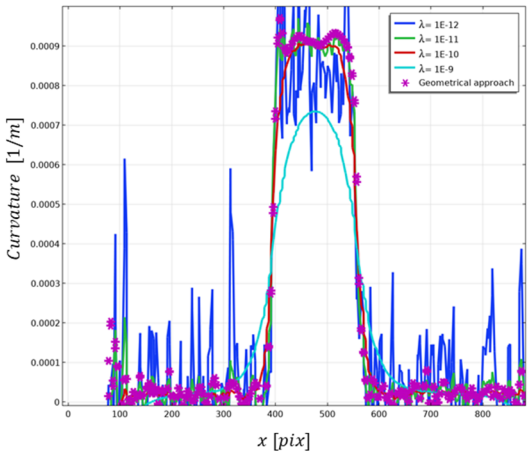

Figure 4. Influence of the tunning parameter λ on the local curvature

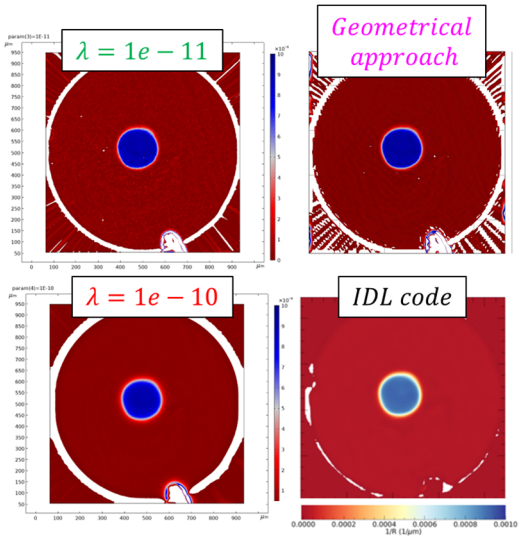

Figure 5. Local curvature computations for two values of λ (left), with the geometrical approach (up right) and with another code (IDL code, bottom right)

With all these validations, the approach adopted for the following optimization procedure is the "tunning approach" (with $\lambda = 1e-11$), providing greater flexibility for further development.

Study Case for β parameter calibration

In order to validate the use of the topologic optimization, a study case has been produced and shown here. The objectives are to calibrate the β parameter and to study the precision of the approach. A direct mechanical problem is solved and illustrated in Figure 6. A load pressure is applied on a surface (top left in Figure 6) and the resulting vertical deformation w_{init} is computed and plotted (top right Figure 6). To study the relevance of the optimization procedure, the inverse problem is solved. By knowing the resulting deformation w_{init}, the objective is to find the optimized load on the loading surface (θ distribution, bottom left in Figure 6), that is required to obtain the same deformation (bottom right in Figure 6).

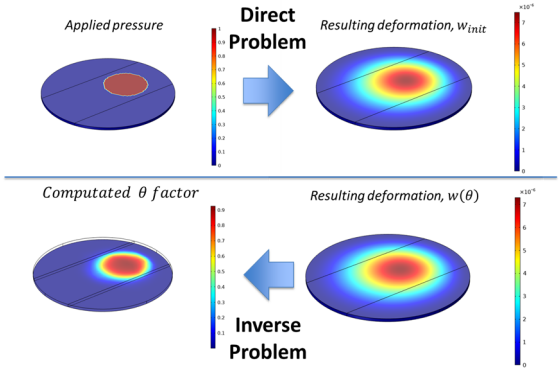

Figure 6. Direct problem results at the top: resulting deformation (right) with the associated applied pressure (left). Inverse problem results at the bottom: resulting deformation (right) and calculated θ factor (left).

Results are compared in Figure 7 for two values of the β parameter controlling the intensity of the optimization projection. The difference between the reference deformation w_{init} and the actual deformation $w(\theta)$ is shown on the left in Figure 7. The relative error is calculated, giving 0.6% of error with $\beta = 1$ and 0.4% of error with $\beta = 8$.

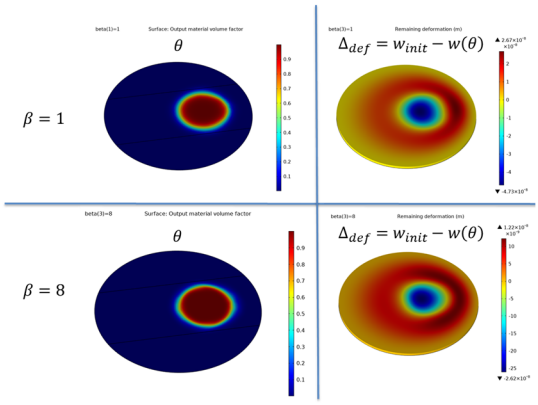

Figure 7. θ factor and Δ_{def} for two values of β

Results are in sufficiently good agreement between the optimized load (top left in Figure 7) founded to obtain the required deformation. A value of $\beta = 8$ is thus chosen to obtain more precision for the following developments.

Results

Surface Flattening with Topologic Optimization

After conclusive numerical validations, the topologic optimization procedure is used on a real surface. The initial calculated curvature of the glass is shown at the top in Figure 8. After 1h of computational time, the resulting optimized curvature is shown at the bottom in Figure 8.

Very good results are obtained in term of local curvature minimization. The initial surface includes areas of high and varying curvatures. The optimized local curvature appears to be very flat and with an amplitude close to 0 over almost the entire surface of the disc.

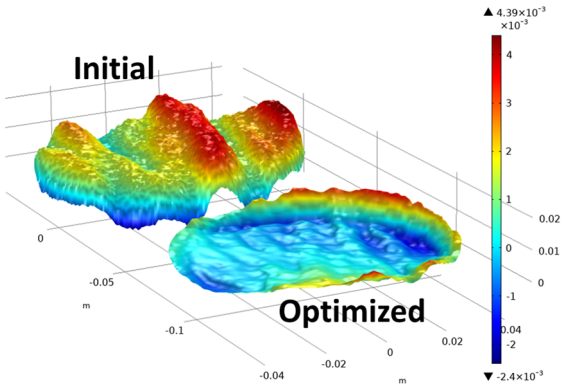

Figure 8. Initial and Optimized Local Curvatures

The gain between the initial global objective value and the optimized one is a factor of 20. This approach gives thus very promising results. Indeed, it gives a continuous representation of the ideal localization of the actuators with the θ factor distribution (as shown in Figure 9). Depending on the rigidity of the glass plate and on the initial curvature, actuators should press harder near the flange (controlling the fixed constraint) than at the center of the disc to compensate the deformation. This continuous approach provides an ideal load distribution minimizing curvature and will be used to set more precisely the actuators position.

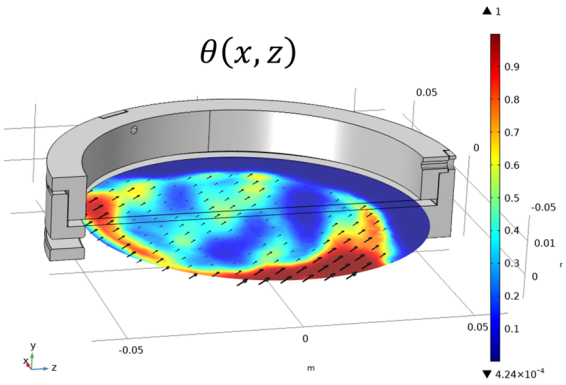

Figure 9. Optimized Load Distribution

Surface Flattening with Parametric Optimization

The second optimization method is also investigated in this paper. As explained previously, the distribution of the actuators is now imposed by setting a certain pattern - with a pitch and a density - as shown on the right in Figure 2. The control variables are the applied loads on each actuator.

An example of obtained results is shown in Figure 10. It gives the values of the intensity of the normalized loads for each actuator K_f (at the top, Figure 10) and the optimized curvature (at the bottom right, Figure 10) compared to the initial curvature (at the bottom left , Figure 10). After 17 iterations, a gain factor of 16 is obtained concerning the optimized curvature, validating the approach implemented.

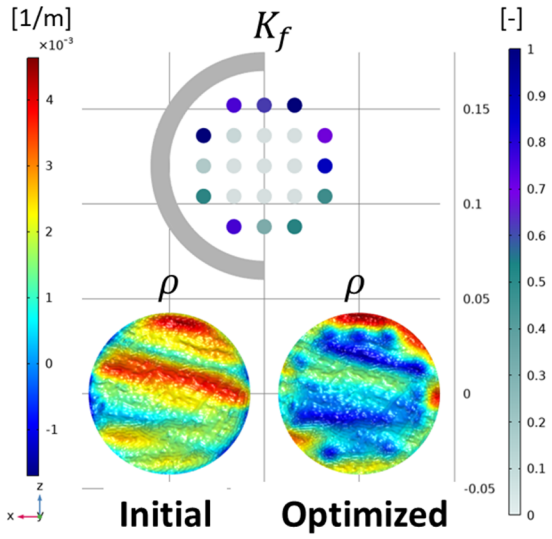

Figure 10. Initial and Optimized Local Curvatures

In a future project, the position of the actuators will also be a degree of freedom, with the aim of also optimizing their position relative to each other. However, the model is still very appropriate to study the influence of actuator positions for different diameter or pitch between them. To simplify the use of the model and to automate the building of each actuator, the Application Builder® is used.

Use of Simulation Application

Thanks to the Application Builder®, a simulation application has been developed and compiled in an executable file. It allows to import a .txt file that can be adjusted in the application before computing the local curvature. Cut lines and postprocessing of the curvature are plotted and can be exported (see Figure 11).

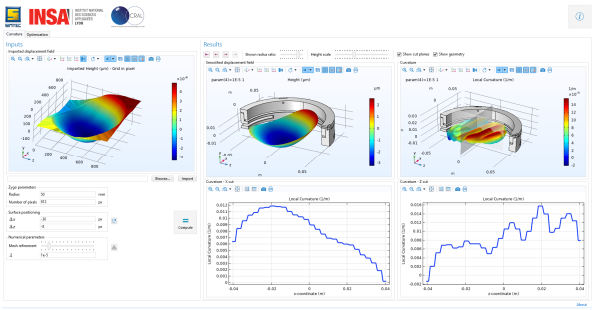

Figure 11. Snapshot of the Application – Local curvature computations

In a second tab, the optimization procedure of the mechanical problem can be used. By defining the radius of the actuators and the distance between them (considered as constant), a pattern is automatically built. The mesh can be adapted in the application to study its influence on the results. In terms of postprocessing, the resulting loads and local curvature are calculated. The gain of the procedure is shown, and the optimized loads of each actuator can be exported in a .txt file.

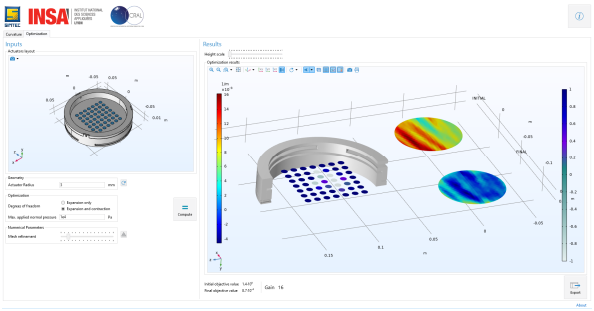

Figure 12. Snapshot of the Application – Optimization procedure

Further developments are in progress to enable the position of the actuators to be defined more freely. In a second phase, the position of the actuators will also be a degree of freedom for the optimization process, providing the optimum position of each actuator for a given actuator radius.

Conclusions

Based on height measurements, two different methods have been implemented to calculate the

local curvature of the latter. After numerical validation, the smoothing method was used for the optimization procedure. To meet two different objectives, two optimization methods, adapted to a mechanical problem, were studied. Both were validated by comparing the optimized curvatures with the curvature of the initial surface, which produced significant gains. Finally, an application was developed to enable the model to be deployed and used for various parametric studies.

Acknowledgments

This project is sponsored by ANR (The French National Research Agency): Project #ANR-18-CE42-0007-01 (Live-Mirror project).

References

[1] K. Thetpraphi, "3D-printed electroactive polymer force-actuator for large and high precise optical mirror applications," *Additive Manufacturing,* vol. 47, 2021.

[2] *Comsol Multiphysics User's Guide, 2022.*